www.amlett.com, www.vbripress.com/aml, DOI: 10.5185/amlett.2015.5933 Published online by the VBRI Press in 2015

Studies of the interaction of bovine serum albumin with pyrimidine-annulated spiro-dihydrofuran and its biological activities

Swarup Roy[1], Sintu Ganai[2], Raj Kumar Nandi[3], K. C. Majundar[3*], Tapan K. Das[1*]

[1]*Department of Biochemistry and Biophysics, University of Kalyani, Kalyani 741235, West Bengal, India*
[2]*School of Sciences, Netaji Subhas Open University, Kolkata 700064, India*
[3]*Department of Chemistry, University of Kalyani, Kalyani 741235, West Bengal, India*

[*]Corresponding author. Tel.:(+91) 3473-238373; E-mail: tapankumardas175@gmail.com (T.K. Das);
Tel.: (+91) 33-2582-7521; E-mail: kcmklyuniv@gmail.com (K.C. Majundar)

Received: 02 April 2015, Revised: 27 June 2015 and Accepted: 09 July 2015

ABSTRACT

The interaction between pyrimidine-annulated spiro-dihydrofuran (PSDF) with bovine serum albumin (BSA) was investigated following spectroscopic studies. The results indicate that dynamic quenching contributes to the fluorescence quenching of BSA by PSDF. The binding constant (K) and the number of binding sites (n) were calculated from the recorded spectra. Based on the Förster's non-radiative energy transfer theory, the average binding distance between BSA and PSDF was estimated. The synchronous fluorescence spectra and circular dichroism indicate that the conformation of BSA has been subjected to alteration in presence of PSDF. The thermodynamic parameters namely ΔH, ΔG, ΔS were calculated at different temperatures (20 ^{o}C, 30 ^{o}C, and 40 ^{o}C) and the results indicated van der Waals force and hydrogen bonding were predominantly present. The compound PSDF also found to exhibit antifungal activity against *Aspergillus* sp. In addition, the results obtained from molecular modeling calculation vividly elucidate the binding mode and the binding sites and results were not well in agreement with the experimental observations. Copyright © 2015 VBRI Press.

Keywords: PSDF; BSA; UV-Vis spectroscopy; quenching; docking.

Introduction

Biomolecules-drug interaction plays an important role in medicinal chemistry and biology. Now a days small molecule-biomolecules interaction has been a hot topic in the field of drug discovery. Interaction between small molecule and biomolecules especially protein [**1-3**] has motivated interdisciplinary research involving both synthetic and analytical chemists as well as biochemists to ascertain the biological function of a small molecules. Several studies have been reported on the fluorescence quenching of proteins induced by some organic compounds with different substituents. Serum albumin, as the most abundant protein in blood plasma, functions as a carrier for various endogenous and exogenous ligands such as fatty acids, hormones, and foreign molecules including drugs [**4**]. So, serum albumin has an important role in the distribution, maintain free osmotic free concentration, excretion, metabolism and interaction with the target tissues of these ligands [**5**]. Bovine serum albumin has been used as a model protein in several biophysical, biochemical and physicochemical studies for many years because of its structural homology with human serum albumin [**6**]. Weak binding leads to a short life time or poor distribution of ligands, whereas strong binding decreases the concentration of free ligands in plasma [**7**]. Consequently, investigations on the interaction mechanisms of ligands to serum albumin may provide some useful information regarding the therapeutic effectiveness of drugs in pharmacology and pharmacodynamics [**8**]. Moreover, an understanding of the chemistry of various classes of pharmaceutical interactions with BSA may culminate into new approaches to drug design and drug therapy [**9**]. In recent years, the interactions of many drugs with BSA were studied [**10-12**].

Pyrimidine, being a component of nucleic acid, exhibits diverse role in biological, pharmaceutical as well as agrochemical sectors. Pyrimidines are important structural components of analogs or precursors of purine bases. It is well established that furo [2, 3-*d*]-pyrimidine [**13**] and spiro-pyrimidine [**14**] derivatives have desirable pharmacological properties. Among them, the furo [2, 3-*d*]-pyrimidine derivatives act as antiulcer agents, muscle relaxants, antihistamines and diuretics [**15**]. Recently, pyrimidine compounds have attracted enormous attention from researchers and are widely recognized as biologically

useful systems because of their potential biological activities, such as antibacterial, antimicrobial, and anticancer, activities [**16, 17**]. Pyrimidine-annulated spiro-dihydrofurans have already been synthesized [**18**].

In order to determine the affinity of PSDF to BSA, we undertook a study to investigate the thermodynamics of their interaction, using fluorescence spectroscopy. Circular dichroism spectra have also been carried out to investigate any structural modification of biomolecules in presence of our compound of interest. Determination of the distance between BSA as donor and PSDF as acceptor was also evaluated by means of the Förster's resonance energy transfer theory. Antifungal activity of PSDF was also studied. Moreover, utilization of molecular modeling was made in order to improve the understanding of the interaction of PSDF with BSA.

Experimental

Material

The Pyrimidine-annulated spiro-dihydrofurans (PSDF) required for this study was prepared according to published procedure [**18**], shown below (**Scheme1**).

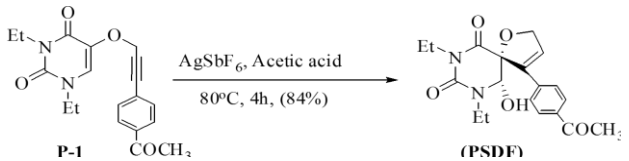

Scheme 1. Preparation of Pyrmidine-ammulated spiro-dihydrofuran.

Bovine Serum Albumin (Sigma) was used in this experiment. The stock solution of BSA was prepared by dissolving BSA in a Tris-HCl (50 mM, pH 7.4) buffer to obtain the concentration of 0.1 µM. Synthesized PSDF (1 mM) was dissolved in methanol. All the other chemicals were of analytical reagent grade and double distilled water was used for all the experimental work.

Apparatus

Fluorescence spectra were recorded on Agilent Technologies Cary-Eclipse Spectrofluorimeter well equipped with attached Cary Temperature controller. The absorption spectra were obtained from a Cary 100 UV-VIS Spectrophotometer (Agilent Technologies). Circular dichroism was recorded in Jasco J-815 CD spectrometer.

Methods

UV–Visible spectroscopy: Spectral changes of BSA was monitored after adding different concentrations of PSDF (0-20 µM) in the range of UV–Visible absorption. The absorption spectra were recorded from 230 to 330 nm at 303K. All the experiments were carried out in Tris-HCl (50 mM, pH 7.4) buffer in a conventional quartz cell.

Intrinsic fluorescence: 3 mL solution containing 0.1 µM BSA was titrated by successive addition of 0-240 µM final concentration of PSDF. Fluorescence spectra were measured in the range of 280-500 nm at the excitation wavelength of 279 nm. The fluorescence spectra were recorded at three temperatures (20 ^{o}C, 30 ^{o}C, and 40 ^{o}C). The range of synchronous scanning were λex = 240, λem (a) = 255, λem (b) =300 nm, where the differences in the wavelengths (Δλ) were 15 and 60 nm, respectively.

Circular dichroism (CD) spectra: The far-UV CD region (190–260 nm), which corresponds to peptide bond absorption, was analyzed to emphasize the content of the regular secondary structure in BSA. Protein solutions were prepared in Tris-HCl (50 mM, pH 7.4) buffer. Protein solutions of 0.01 µM were used to obtain the spectra. Spectral changes of BSA were monitored after adding PSDF (0-25 µM).

Antimicrobial activity: Czapek Dox broth (pH 7.4) was used as growth medium. Agar medium surface was cut by using sterile gel borer to make wells (5 mm diameter). The synthetic compound PSDF was used to study the antifungal activities against the fungal strains of *Aspergillus* sp like *Aspergillus niger*, *Aspergillus foetidus* & *Aspergillus parasiticus*.100 µl of PSDF (100 µg/ml) were poured into separate wells. Plates were incubated at 30 ^{o}C and zone of inhibition was measured after 48 h [**19**]. Silver nanoparticles (SNP) have been biologically synthesized using a fungi *Aspergillus foetidus* and 100 µg/ml was tested in order to account for the antifungal activity. The details of biosynthesis, characterization of SNP have already been reported [**19, 20**]. Also activity of this synthetic compound was examined in conjugation with the biosynthesized SNP to witness the synergic effect of both SNP and PSDF. For the combination study we mixed equal amounts of both at a same concentration, maintaining other conditions as stated previously.

Molecular docking: The crystal structure of BSA was obtained from the Protein Data Bank (entry code 4F5S). The Auto Dock 4.0 [**21**] was employed to compute the possible binding mode of the PSDF with BSA. The 3-D structure of PSDF and BSA was modeled on molecular modeling software discovery digital studio 4.0. The docking calculations were then performed using the Lamarckian genetic algorithm (LGA) for ligand conformational searching. Lamarckian genetic algorithm implemented in the auto dock was used to estimate the possible binding conformations of PSDF. During the docking process, a maximum of 10 different conformations were considered for the PSDF. The conformer with the lowest binding free energy was used for further analysis.

Results and discussion

Absorption characteristics of BSA-PSDF interaction

Fig. 1. shows the absorption spectra of BSA and BSA in the presence of increasing concentration of PSDF. It was found in **Fig. 1.** that as the PSDF concentration increases; the intensity of the wavelength at 279 nm increases significantly with a blue shift. UV-Vis spectra of PSDF were also studied in different solvent (**Supplementary Fig. S1**) such as acetonitrile, chloroform, acetone, DMF, methanol. The compound PSDF showed highest

absorbance in chloroform but in all solvent the nature of spectrum was very similar.

This increase in intensity is suggestive of the formation of the ground state complex between BSA and PSDF. Also we have checked the effect of solvent methanol on BSA and we observed no significant changes in absorption spectra upon addition of solvent. The equilibrium for the formation of complex between BSA and PSDF is given by Eq. 1, values of the apparent association constant, K_{app}, were obtained from the BSA absorption at 279 nm according to the methods of Benesi and Hildebrand equation published in the literature [**22**].

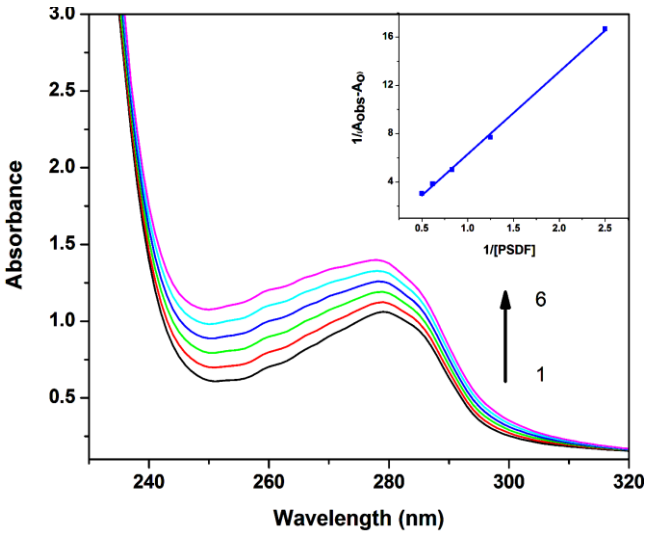

Fig. 1. Absorption spectra of BSA (0.1 µM) in presence of PSDF (1-6): (0, 4, 8, 12, 16 and 20 µM), **Fig. 1(inset)** Calculation of K_{app} of BSA - PSDF complex; $1/(A_{obs}-A_0)$ *vs* 1/[PSDF] plot.

$$\frac{1}{A_{obs}-A_0}=\frac{1}{A_C-A_0}+\frac{1}{K_{app}(A_C-A_0)[PSDF]} \quad (1)$$

where, A_0 is the absorbance of BSA in the absence of PSDF and A_C is the recorded absorbance at 279 nm for BSA at different PSDF concentrations. The double reciprocal plot of $1/(A_{obs}-A_0)$ *vs* 1/[PSDF] is linear and the apparent association constant (K_{app}) was determined to be 4.9×10^3 (R= 0.9992, where R is the correlation coefficient) [**Fig. 1. inset**] from the ratio of the intercept to the slope [**22**]. The value of K_{app} is considerably small, thereby indicating formation of a weak complex between BSA and PSDF.

Characteristics of fluorescence spectra

Fig. 2 shows the fluorescence emission spectra of BSA and BSA mixed with PSDF [**23**]. It is observed that with the increase in PSDF concentration the emission intensity decreases. Quenching can be induced by different mechanisms, which are usually classified as dynamic quenching and static quenching [**24**]. The quenching data can be described by the Stern Volmer equation [**24, 25**].

$$F_0/F=1+K_q\tau_0[Q]=1+Ksv[Q] \quad (2)$$

where, F_0 and F represent the fluorescence intensities in the absence and presence of quencher, K_q is the bimolecular quenching rate constant, K_{SV} is the Stern Volmer constant, τ_0 is the average lifetime of the molecule without quencher and [Q] is the concentration of the quencher. Since the fluorescence lifetime of a biopolymer is 10^{-8} s [**24**], the K_q values were calculated using the formula $K_q= K_{SV}/\tau_o$.

In case of dynamic quenching the maximum scatter quenching collision constant of various quenchers with the biopolymer is near 1×10^{10} L/mol/s [**24**]. Quenching data can be presented as plots of F_0/F *vs* [Q]. A plot of F_0/F *vs* [Q] yields a slope equal to Stern Volmer quenching constant. The values of K_{SV} and K_q at different temperatures are shown in **Table 1**. The linearity of the F_0/F *vs* [Q] plots has been depicted in **Fig. 2 inset**.

As shown in **Table 1** (**Supporting information**), the quenching constant K_{SV} increases with the increase in temperature from which it can be inferred that the probable quenching mechanism operative in case of BSA is dynamic in nature [**26-29**].

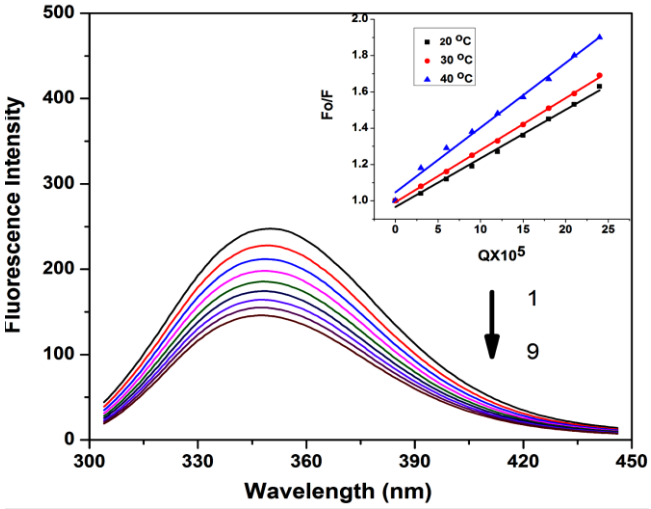

Fig. 2. Fluorescence quenching spectra of BSA by PSDF, λ_{ex} = 279 nm; $C_{(BSA)}$ = 0.1 µM; $C_{(PSDF)}$ (1-9): (0, 30, 60, 90, 120, 150, 180, 210, and 240 µM), **Fig. 2 inset**: Stern Volmer plot for PSDF and BSA at 20°C, 30°C, and 40°C respectively.

Binding constant (K) and number of binding sites (n)

The number of binding sites (n) and the binding constant (K) between PSDF and BSA have been calculated using the Eq.3 [**30**].

$$log\frac{F_o-F}{F}=logK+n\log[Q] \quad (3)$$

A plot of log $[(F_0-F)/F]$ *vs* log [Q] gives a straight line, whose slope equals to n and the length of intercept on Y-axis equals to log K.

Fig. 3 illustrates the double logarithmic plots and **Table 2** gives the corresponding results. The values of 'n' (**Table 2**) at the experimental temperatures were ~1 which is indicative of a single binding site on BSA for PSDF and the binding phenomenon can be attributed to be a temperature dependent process within the range 20 to 40 °C.

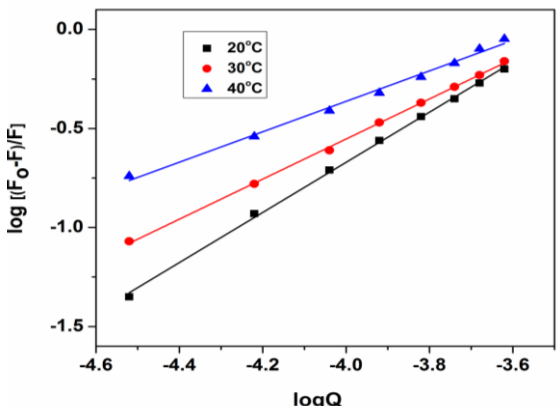

Fig. 3. Plots of the PSDF quenching effect on BSA fluorescence at 20 °C, 30 °C, and 40 °C.

From **Table 2**, it was observed that with increase in temperature the binding constant K decreases which thereby illuminates the fact that the stability of the PSDF-BSA complex considerably weakens with the enhancement of temperature.

Table 2. Binding constants (K) and number of binding sites (n) on BSA for PSDF.

T(°C)	R[a]	K (L/mol)×10^3	n
20	0.9994	24.5	1.26
30	0.9996	3.09	1.01
40	0.9968	0.51	0.77

[a]correlation coefficient.

Thermodynamic parameters and nature of binding forces

The possible interactions operative between two molecules are hydrogen bonding, van der Waals forces, hydrophobic, hydrophilic and electrostatic interactions. If the enthalpy changes (ΔH) does not vary significantly over the temperature range studied, then the thermodynamic parameters ΔH (enthalpy change) and ΔS (entropy change) can be determined using the Van't Hoff Eq. (Eq. 4), where K is the binding constant at the corresponding temperature (**Fig. 4**). ΔH and ΔS can be determined from the slope and intercept of linear Van't Hoff plot. The Gibbs free energy change (ΔG) is obtained from the Eq. 5.

$$\ln k = -\Delta H / RT + \Delta S / R \quad (4)$$

$$\Delta G = \Delta H - T\Delta S = -RT \ln K \quad (5)$$

According to the enthalpy and entropy changes, the mode of interaction between small molecules and biomolecules can be summarized as ΔH>0 and ΔS>0: indication of hydrophobic forces; ΔH<0 and ΔS<0: indication of van der Waals interactions and hydrogen bonds; ΔH≈0 and ΔS>0: indication of electrostatic interaction [**31**]. The Eq. 4 yields the values of ΔH and ΔS to be -160.87 kJ/mol and -463.25 J/mol/K respectively for PSDF-BSA complex. The values of the thermodynamic parameters ΔH, ΔS and ΔG are mentioned in **Table 3**. As shown in **Table 3**, ΔG, ΔH, and ΔS were negative. Therefore, the data obtained manifests the spontaneity of the formation of PSDF-BSA complex and simultaneously claiming it to be an exothermic reaction accompanied by a negative ΔS value.

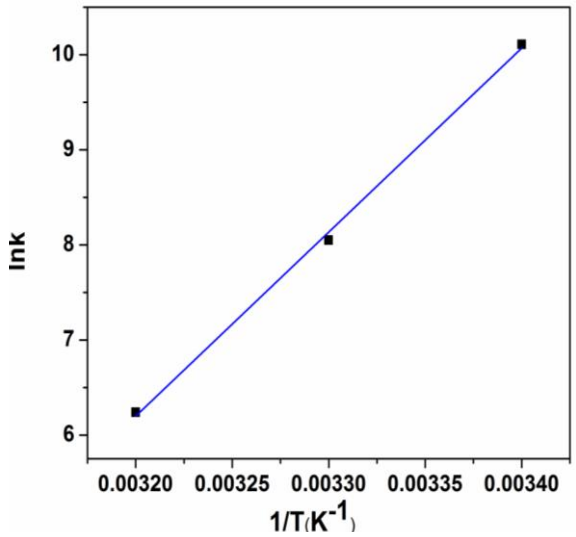

Fig. 4. The Van't Hoff plot for the interaction of BSA and PSDF.

Table 3. Thermodynamic parameters for the binding of the PSDF to BSA at different temperature.

T(°C)	R[a]	ΔH (kJ/mol)	ΔS (J/mol/K)	ΔG (kJ/mol)
20	0.9993	-160.87	-463.25	-25.20
30	0.9993	-160.87	-463.25	-25.20
40	0.9993	-160.87	-463.25	-25.20

[a]correlation coefficient.

According to previous report of Neméthy and Scheraga [**32**], Ross and Subramanian [**30**], the value suggested that van der Waals force and hydrogen bonding were responsible for this type of interaction. The negative value of ΔG revealed that the interaction process was spontaneous. Accordingly, it was likely that weak forces were involved in the binding phenomenon. Similar results were also observed in previous reports [**33-36**].

Synchronous fluorescence spectra

A synchronous fluorescence spectrum provides knowledge about the molecular environment in the vicinity of the fluorophores functional group. The value of Δλ i.e. difference between excitation and emission wavelengths is an important operating parameter. According to Miller, [**37**] when Δλ=15 nm, synchronous fluorescence spectrum indicates the changes in the microenvironment of tyrosine residues and when Δλ=60 nm, it provides information regarding the microenvironment of tryptophan residues. It can be seen from the **Fig. 5** (**Supplementary file**), **Fig 5a** shows when Δλ= 15 nm, there is a slight red shift in emission wavelength of tyrosine and in case of Δλ= 60 nm (**Fig. 5b**) no changes of shifting in λmax was observed. The red shift of tyrosine indicates polarity around tyrosine residues is increased and the hydrophobicity is decreased in the presence of PSDF, indicating PSDF induces conformational changes in BSA [**7**].

Circular dichroism spectroscopy

The CD spectra of BSA exhibited two negative minima at 208 nm and 222 nm, which is typical characterization of the helix structural class of proteins [**38**]. **Fig. 6** (**Supplementary file**) shows the helicity of BSA in the presence of increasing concentration of PSDF. In the wavelength region of 190–260 nm, the CD spectrum of a protein gives information about its conformation in relation to the secondary structure. The binding of PSDF to BSA causes inconspicuous changes to both these bands but it is apparent that the interaction of PSDF with BSA is liable to contribute some conformational change of the protein.

Energy transfer between BSA and PSDF

According to Förster's non-radiative energy transfer theory (FRET) [**39**], the rate of energy transfer depends on three factors: (i) the relative orientation of the donor and acceptor dipoles, (ii) the extent of overlap of the emission spectrum of the donor with the absorption spectrum of the acceptor, and (iii) the distance between the donor and the acceptor. The energy transfer effect is related not only to the distance between the acceptor and the donor, but also to the critical energy transfer distance R_0, as described in Equation 6.

$$E = 1 - \frac{F}{F_o} = R_0^6 / (R_0^6 + r^6) \qquad (6)$$

where, F and F_0 are the fluorescence intensities of BSA in the presence and absence of PSDF, r is the distance between acceptor and donor and R_0 is the critical distance when the transfer efficiency is 50 %, which can be calculated from the Equation 7.

$$R_0^6 = 8.8 \times 10^{-25} k^2 N^{-4} \phi J \qquad (7)$$

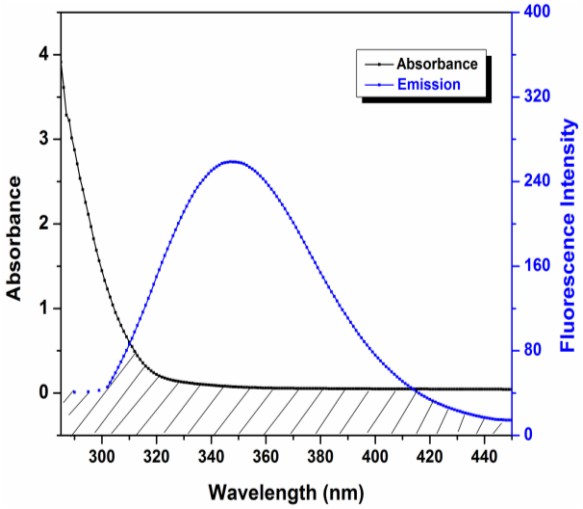

Fig. 7. Overlap plot of the fluorescence emission spectra of BSA (0.1 µM) and the UV-Vis absorption spectra of PSDF (1mM).

Where, k^2 is the spatial orientation factor between the emission dipole of the donor and the absorption dipole of the acceptor. The dipole orientation factor, k^2, is the least certain parameter to be used in the calculation of the critical transfer distance. Although theoretically k^2 can vary from 0 to 4, the extreme values require very rigid orientations. If both the donor and acceptor are tumbling rapidly and free to assume any orientation, k^2 equals 2/3. If only the donor is free to rotate, k^2 can vary from 1/3 to 4/3 [**23**]. N is the refractive index of the medium, ϕ is the fluorescence quantum yield of the donor and J is the overlap integral of the fluorescence emission spectrum of the donor and the absorption spectrum of the acceptor given by the following Equation 8.

$$J = \sum F(\lambda)\varepsilon(\lambda)\lambda^4 \Delta\lambda / \sum F(\lambda)\Delta\lambda \qquad (8)$$

where, F (λ) is the fluorescence intensity of the fluorescent donor at wavelength λ and is dimensionless; ε (λ) is the molar absorption coefficient of the acceptor at wavelength λ. J can be evaluated by integrating the spectra in **Fig. 7.** It has been reported for BSA, k^2 = 2/3, ϕ = 0.15 and N = 1.336 [**40**]. Thus, from the Eq. 8 above, J = 9.14×10^{-16} $cm^3\times L/mol$, E = 0.077, R_0 = 1.71 nm, and r = 2.59 nm have been calculated. The average distances between a donor fluorophore and acceptor fluorophore on the 2–7 nm scale [**41**] and $0.5R_0 < r < 1.5R_0$ [**42**] denoted that the energy transfer occurs between BSA and PSDF [**43, 44**], and also indicated that the fluorescence quenching of BSA was a non-radiative transfer process. The binding distance r is much less than 7 nm which implies that the energy transfer occurs between BSA and PSDF with high probability [**44**] and also indicated that the fluorescence quenching of BSA was a non-radiative transfer process.

Antifungal activity

The zone of inhibition caused by the PSDF is shown in **Fig. 8** (**Supplementary file**). Further the PSDF are found to be toxic against fungi at concentration of 100 µg/ml (Shown in **Table 4** as supporting information). As SNP possess antimicrobial activity and PSDF showed antifungal activity, struck by curiosity we indulged into examining the effect of combination of SNP with PSDF. It was observed that the antifungal activity slightly increased when both were combined.

Molecular modeling

The fluorescence, UV-Vis, and CD spectroscopic results were complemented with molecular modeling, in which PSDF was docked to BSA to locate the preferred binding site and the binding mode. Molecular docking technique has been employed to understand the different binding modes of BSA-PSDF interaction [**45-47**]. The 3D structure of BSA was obtained from Protein Data Bank. The possible conformations of the BSA-PSDF complex were calculated using Auto Dock 4.0 program. Out of 10 conformers, the conformer with the lowest binding free energy was used for further analysis.

The best energy ranked model (**Fig. 9**(**a**)) revealed that the PSDF bound at the interface between two sub domains IIA and IIIA, which is located just above the entrance of the binding pocket of IIA. In **Fig. 9**(**b**), PSDF molecule was found to be surrounded by 13 amino acid residues within a distance of 5 Å: 8 hydrophobic residues (Phe506,

Phe567, Phe553, Phe508, Ala510, Ala568, Val575, Gly571) 3 hydrophilic residues (His509, Pro572, Thr507) and only 2 ionic residues (Glu503, Glu564). Therefore, it can be concluded that the interaction between PSDF and BSA is dominated by hydrophobic forces and van der Waals interactions indicating the possibility of interaction between PSDF and BSA.

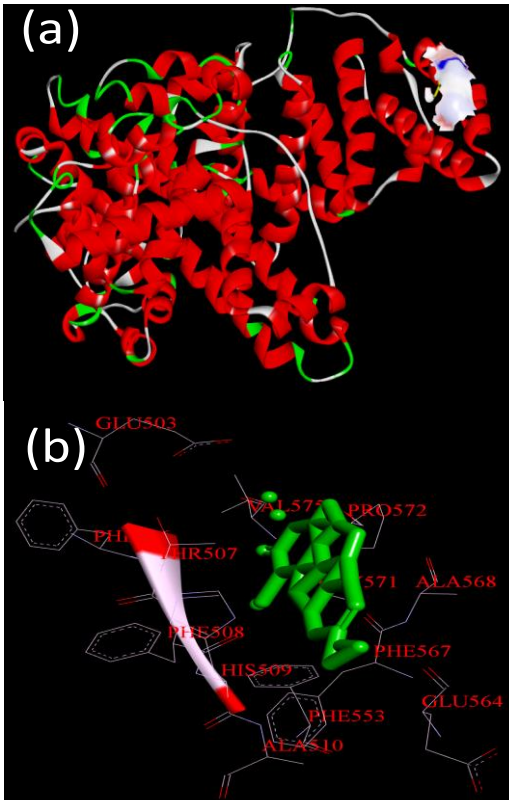

Fig. 9. Best conformation for PSDF docked to BSA, a) place of interaction of PSDF and BSA and b) The surrounding amino acid residues of BSA within 5Å from PSDF (green colored).

But, this theoretical result is not fully agreement with the experimental result. A possible reason for this may be that the X-ray structure of the BSA from crystals is different from that of the aqueous system used. So, this theoretical study indicated the binding of PSDF to BSA.

Conclusion

The reactivity of PSDF towards BSA revealed that the quenching of BSA fluorescence is dynamic in nature, where van der Waals force and hydrogen bonding are thought to be responsible for their complexation. The binding distance of PSDF with BSA was calculated to be 2.59 nm, on the basis of FRET, which indicates that the energy transfer can occur with ease. The antifungal activity studies demonstrate that the compound (PSDF) exhibits antifungal activity against *Aspergillus* sp. whereby a slight increase in the so-called activity is also evident upon combination with SNP. Molecular docking study confirms the interaction between the PSDF and BSA. It is expected that this study may provide important insight into further investigations of PSDF molecule for its future application as pharmaceuticals.

Acknowledgements

S.R is thankful to the Department of Science Technology (DST) of India, for a DST INSPIRE fellowship (IF110421). R. K. N. and S.G. are grateful to CSIR (New Delhi) for their research fellowships. S.G is also grateful to Netaji Subhas Open University, Kolkata for constant support.

Author contributions

Conceived the plan: SR; Performed the expeirments: SR; Data analysis: SR; Wrote the paper: SR, TKD, SG, RKN, KCM (SR, TKD, SG, RKN, KCM are the initials of authors). Authors have no competing financial interests.

Reference

1. Froehlich, E.; Mandeville, J. S.; Jennings, C. J.; Sedaghat-Herati, R.; Tajmir-Riahi, H. A. *J. Phys. Chem. B*; **2009**, *113*, 6986. **DOI:** 10.1021/jp9011119
2. Charbonneau, D.; Beauregard, M.; Tajmir-Riahi, H. A. *J. Phys. Chem. B*; **2009**, *113*, 1777. **DOI:** 10.1021/jp8092012
3. Bourassa, P.; Hasni, I.; Tajmir-Riahi, H. A. *Food Chem.*; **2011**, *129*, 1148. **DOI:** 10.1016/j.foodchem.2011.05.094.
4. He, X.M.; Carter, D. C. *Nature*; **1992**, *358*, 209. **DOI:** 10.1038/358209a0
5. Sudhamalla, B.; Gokara, M.; Ahalawat, N.; Amooru, D. G.; Subramanyam, R. *J. Phys. Chem. B*; **2010**, *114*, 9054. **DOI:** 10.1021/jp102730p
6. Tajmir-Riahi, H. A. *J. Iran Chem. Soc.*; **2006**, *3*, 297. **DOI:** 10.1007/BF03245950
7. Zhang, Y.; Zhou, B.; Liu, Y.; Zhou, C.X.; Ding, X.L. Liu, Y. *J. Fluoresc.*; **2008**, *18*, 109. **DOI:** 10.1007/s10895-007-0247-4
8. Kamat, B. P.; Seetharamappa, J. *J. Pharm. Biomed. Anal.*; **2004**, *35*, 655.
9. Dennis, M. S.; Zhang, M.; Meng, Y. G.; Kadkhodayan, M.; Kirchhofer, D.; Combs, D.; Damico, L. A. *J. Biol. Chem.* ; **2002**, *277*, 35035. **DOI:** 10.1074/jbc.M205854200
10. Mandeville, J. S.; Froehlich, E.; Tajmir-Riahi, H. A. *J. Pharm. Biomed. Anal*.; **2009**, *49*, 468. **DOI:** 10.1016/j.jpba.2008.11.035.
11. Bourassa, P.; Dubeau, S.; Maharvi, M. G.; Fauq, A. H.; Thomas, T. J.; Tajmir-Riahi, H. A. *Biochimi.*; **2011**, *93*, 1089. **DOI:** 10.1016/j.biochi.2011.03.006.
12. Belatik, A.; Hotchandani, S.; Bariyanga, J.; Tajmir-Riahi, H.A. *Eur. J. Med. Chem.*; **2012**, *48*, 114. **DOI:** 10.1016/j.ejmech.2011.12.002.
13. Clercq, E. De. *Med. Res. Rev.*; **2003**, *23*, 253. **DOI:** 10.1002/med.10035
14. Mangiavacchi, S.; Calistri, M. T. *Ann. Chim.*; **1973**, *63*, 883. **ISSN:** 1612-8877
15. Melik-Ogandzhanyan, R. G.; Khachatryanand, V. E.; Gapoyan, A. S. *Russ. Chem. Rev.*; **1985**, *54*, 262. **DOI:** 10.1070/RC1985v054n03ABEH003026
16. Li, X.; Zheng, A.; Liu, B.; Yu, X.; Yi, P. *Chin. J. Chem.*; **2010**, *28*, 977. **DOI:** 10.1002/cjoc.201090181
17. Amr, A. E.-G. E.; Maigali, S. S.; Abdulla, M. M. *Monatsh. Chem.*; **2008**, *139*, 1409. **DOI:** 10.1007/s00706-008-0937-x
18. Majumdar, K. C.; Ganai, S.; Nandi, R. K.; *New J. Chem.*; **2011**, *35*, 1355. **DOI:** 10.1039/c1nj20121b
19. Majumdar, K. C.; Ponra, S.; Ghosh, T. Synthesis, **2013**, 3164. **DOI:** 10.1055/s-0033-1338533
20. Roy, S.; Mukherjee, T.; Chakraborty, S.; Das, T. K. *Dig. J. Nanomater. Biostruct.*; **2013**, 8, 197. **ISSN:** 1842-3582
21. Roy, S.; Das, T. K. *Nanosci. Nanotechnol. Lett.*; **2014**, 6, 181. **DOI:** 10.1166/nnl.2014.1749
22. Morris, G. M.; Goodsell, D.S.; Halliday, R.S.; Huey, R.; Hart, W.E.; Belew, R.K.; Olson, A.J. Autodock, version 4.0.1 LaJolla, CA: The Scripps Research Institute, **2007**.
23. Stephanos, J. J. *J. Inorg. Biochem.* **1996**, 62, 155. **ISSN:** 0162-0134

24. Jhonsi, M. A.; Kathiravan, A.; Renganathan, R. *Colloids Surf. B*; **2009**, *72*, 167. **DOI:**10.1016/j.colsurfb.2009.03.030
25. Lakowicz, J. R. *3rdedn, Principle of fluorescence spectroscopy*, Springer, New York. **1999**. **ISBN:** 978-0-387-46312-4
26. Wang, R.; Chai, Y.; Wang, R.; Zhang, L.; Wu, J.; Chang, J. *Spectrochim. Acta A*.; **2012**, *96*, 324. **DOI:** 10.1016/j.saa.2012.05.030
27. Roy, S.; Das, T. K. *J Nanosci. Nanotechnol*.; **2014**, *14*, 4899. **DOI:** 10.1166/jnn.2014.9508.
28. Shi, Y.; Liu, H.; Xu, M.; Li, Z.; Xie, G.; Huang, L.; Zeng, Z. *Spectrochim. Acta A*.; **2012**, *87*, 251. **DOI:**10.1016/j.saa.2011.11.048
29. Roy, S.; Das, T. K. *Nanosci. Nanotechnol. Lett*.; **2014**, *6*, 547. **DOI:** 10.1166/nnl.2014.1852
30. Roy, S.; Sadhukhan, R.; Ghosh, U.; Das, T. K. *Spectrochimica Acta A*.; **2015**, *141*, 176. **DOI:** 10.1016/j.saa.2015.01.041
31. Kandagal, P. B.; Ashoka, S.; Seetharamappa, J.; Shaikh, S. M. T.; Jadegoud, Y.; Ijare, O. B.; *J Pharm. Biomed. Anal.*; **2006**, *41*, 393. **DOI:**10.1016/j.jpba.2005.11.037
32. Ross, D. P.; Subramanian, S. *Biochemistry*; **1981**, *20*, 3096. **DOI:** 10.1021/bi00514a017
33. Neméthy, G.; Scheraga, H. A. *J. Phys. Chem;* **1962**, *66*, 1773. **DOI:** 10.1021/j100816a004
34. Yu, X.; Liao, Z.; Yao, Q.; Liu, H.; Li, X.; Yi, P. *Spectrochim. Acta A*; 2014, *118*, 331. **DOI:** 10.1016/j.saa.2013.08.103
35. Wangn, R.; Dou, H.; Yin, Y.; Xie, Y. Sun, L.; Liu, C.; Dong, J.; Huang, G.; Zhu, Y.; Song, C.; Chang, J. *J. Luminesce*.; **2014**, *154*, 8. **DOI:** 10.1016/j.jlumin.2014.04.001
36. Yu, X.; Liao, Z. Yao, Q.; Liu, H.; Xie, W. *Spectrochim. Acta A*; **2014**, *127*, 231. **DOI:** 10.1016/j.saa.2014.02.064
37. Xu, C.; Gu, J.; Ma, X.; Dong, T.; Meng, X. *Spectrochim. Acta A*; **2014**, *125*, 391. **DOI:** 10.1016/j.saa.2014.01.132
38. Fuller, C. W.; Miller, J. N. *Proc Anal Div Chem Soc*.; **1979**, *16*, 199. **DOI:** 10.1039/AD9791600199
39. Hu, Y. J.; Liu, Y.; Shen, X. S.; Fang, X.Y.; Qu, S. S. *J. Mol. Struct.*; **2005**, 738, 143. **DOI:**10.1016/j.molstruc.2004.11.062
40. Förster, T. *Mod. Quantum Chem., Third ed.*, Academic, New York, **1996**.
41. Cyril, L.; Earl, J. K.; Sperry, W. M. *Biochemist's Handbook*, E. & F.N. Spon, London, **1961**.
42. Weiss, S. *Science* 1999, *283*, **1676**. **DOI:** 10.1126/science.283.5408.1676
43. Valeur, B. *Molecular Fluorescence: Principles and Applications*, Wiley, New York, **2001**. **ISBN:** 3-527-60024-8
44. Kyhm, K.; Kim, I.; Kang, M.; Woo, H. Y. *J Nanosci. Nanotechnol*.; **2012**, *12*, 7733. **DOI:** 10.1166/jnn.2012.6633
45. Valeur, B.; Brochon, J. C. *New Trends in Fluorescence Spectroscopy*, Springer Press, Berlin; **2001**.
46. Gao, W. H.; Li, N.; Chen, Y.W.; Xu, Y.; Lin, Y.; Yin, Y.; Hu, Z. *J. Mol. Struct*.; **2010**, *983*, 133. **DOI:**10.1016/j.molstruc.2010.08.042
47. Paal, K.; Shkarupin, A.; Beckford, L. *Bioorg. Med Chem*.;**2007**, *15*, 1323. **DOI:**10.1016/j.bmc.2006.11.012
48. Fahimeh, J.; Parisa S. D.; Hamid, M. *J. Lumin.;* **2014**, *148*, 347. **DOI:** 10.1016/j.jlumin.2013.12.046

Supporting information

Preparation of pyrimidine-annulated spiro-dihydrofuran

The non-terminal alkyne substrate (P-1) was treated with 10 mol % $AgSbF_6$ in acetic acid at 80 ^oC for 4 h. After completion of the reaction (as monitored by TLC), the reaction mixture was cooled and neutralized with saturated $NaHCO_3$ solution. This was extracted with dichloromethane (3 x 10 mL). The combined organic extract was washed with brine (1 x 10 mL) and dried over Na_2SO_4. The solvent was distilled off. The resulting crude product was purified by column chromatography over silica gel (60-120 mesh) using a petroleum ether-ethyl acetate mixture (2 : 3) as an eluent to get the pyrimidine-annulated spiro-dihydrofuran in 84 % yield. The white solid compound was stable in heat and its melting point was found to be 143-145 ^oC.

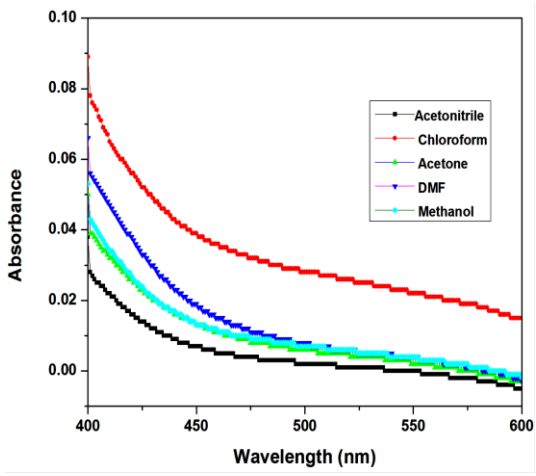

Fig. S1. UV-Vis absorption spectra of PSDF in different solvents (1mM).

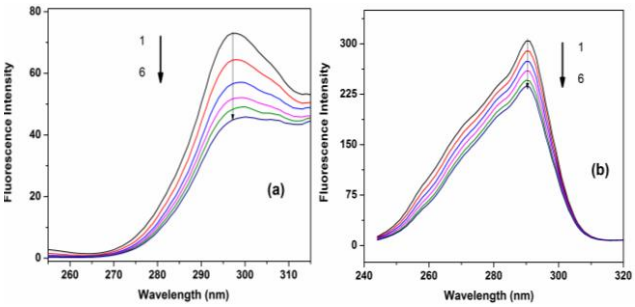

Fig. 5. Synchronous fluorescence spectra of BSA in presence of PSDF at $\Delta\lambda$ =15 nm (a) and $\Delta\lambda$ = 60nm (b), respectively.

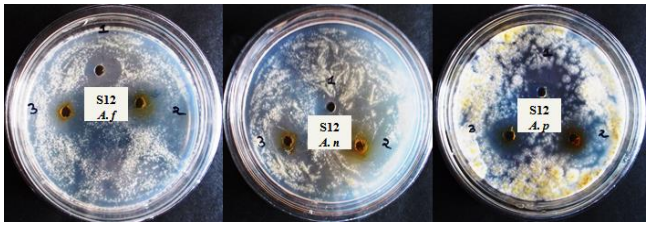

Fig. 8. Antimicrobial activity of PSDF showed against *Aspergillus species* (in plate picture; 1 denotes PSDF, 2 denotes SNP and 3 denotes PSDF+SNP).

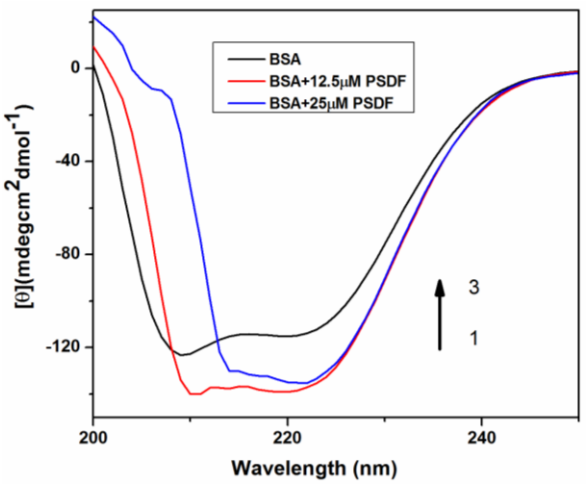

Fig. 6. CD spectra of PSDF-BSA system at the BSA concentration of 0.01 μM and PSDF concentrations of 1: 0, 2: 12.5 μM, 3: 25μM.

Table 1. The Stern–Volmer constants and quenching constants of BSA by PSDF at varying temperatures.

T (°C)	R_a	K_{SV} (L/mol) ×10^{-2}	K_q (L/mol/S)×10^6
20	0.9969	2.67	2.67
30	0.9997	2.86	2.86
40	0.9967	3.56	3.56

Table 4. Antifungal activity of PSDF against *Aspergillus* sp.

Fungi	Zone of inhibition diameter (in mm)		
	PSDF	SNP	PSDF+SNP
Aspergillus foetidus	12	13	14
Aspergillus parasiticus	8	11	12
Aspergillus niger	6	10	15